Simulation Study of the Effect of Modelling Errors on the Solution of Inverse Cardiac Source Imaging Problem Using Realistic Source Patterns

O Skipa, FB Sachse, CD Werner, O Dössel

Institut für Biomedizinische Technik, Universität Karlsruhe (TH), Germany

Abstract

The effect of the modelling errors on the solution of the inverse problem of electrocardiography is investigated. The electrocardiographic signal is simulated using a finite element model of human torso and realistic source patterns gained with a cellular automaton. Noise is added to simulated measurements and the inverse problem is solved. Modelling errors consist of false conductivity assumptions, changed anisotropy ratio of skeletal muscles and geometric errors. The effect of modeling errors on optimal regularization parameter determination is investigated. The changes in muscle anisotropy and heart position are shown to have the highest effect on reconstructed epicardial potentials. CRESO and L-curve criteria for optimal regularization parameter estimation are compared.

1. Introduction

The reconstruction of epicardial potential distributions from measured body surface potential maps (BSPM) plays an important role in noninvasive cardiac source imaging. Methods varying from simple truncated singular value decomposition to complex optimization procedures exist to solve this ill-posed problem. All of these methods require a model of the volume conductor which adequately describes the relation between the source patterns on the epicardial surface and the BSPMs. The creation of a high-quality model is a complex and time-consuming procedure. Therefore, a question of great interest is what level of details the model must include for the reconstruction procedure to be successful. The analysis of modelling errors in forward and inverse bioelectric field problems is still an important research topic [1][2]. In this work we investigate the effect of modelling errors on the inverse solution using a highly detailed finite element model of human body and simulated realistic source patterns gained with a cellular automaton. The errors in assumed conductivity values and variations in skeletal muscles anisotropy ratio as well as the geometric errors are simulated. The effect of the modelling errors on the optimal regularization parameter determination and on the quality of the reconstruction is evaluated.

2. Methods

This section describes the formulation of the forward and inverse electrocardiografic problems, methods for optimal regularization parameter estimation and the numerical simulations performed.

2.1. Forward problem

The construction of transfer matrices and the BSPM simulations require multiple solutions of Poisson's equation for electrical conduction:

$$\nabla \cdot (\sigma \nabla \varphi) = i \qquad (1)$$

where φ is the potential, σ the conductivity tensor and i the impressed source current density $[A/m^3]$. Equation (1) was solved by Finite Element Method (FEM). Finite element model of human torso (Fig. 1) consists of about 800.000 tetrahedrons and includes more than 20 tissue classes as well as fiber orientation in skeletal muscles and myocardium. About 60.000 mesh nodes are placed regularly in the heart to allow for the interpolation of sources gained with a cellular automaton. The finite element model was derived from the MEET Man data set developed at the Institute of Biomedical Engineering, Universität Karlsruhe (TH) [3].

The BSPM simulation starts from computing the transmembrane potentials in the heart with a cellular automa-

Figure 1. Finite element model of human torso.

0276-6547/01 $17.00 © 2001 IEEE

Computers in Cardiology 2001;28:41-44.

ton [4]. The transmembrane potential distributions are simulated for complete cardiac cycle with a given time step. Then the impressed current source density distributions are computed using bidomain model [5] and a series of forward computations is performed to get BSPMs.

2.2. Inverse problem

Discretization of equation (1) leads to a linear relationship between the vector of epicardial potentials x and the vector of body surface potentials b:

$$Ax = b \tag{2}$$

The transfer matrix A describes the geometrical and conductive properties of the torso model. The inverse problem of finding x from b is ill-posed and requires regularization.

For solving the inverse problem, Tikhonov zero-order regularization was used:

$$x_\lambda = arg\ min\{\|Ax - b\|_2^2 + \lambda^2 \|x\|_2^2\}, \tag{3}$$

where λ is the regularization parameter and x_λ is the corresponding approximate solution [6].

Two criteria for *a priori* regularization parameter estimation are popular in connection with inverse electrocardiographic problems: Composite REsidual and Smoothing Operator (CRESO) [7] and L-curve [8]. CRESO criterion delivers optimal λ_C as a first relative maximum for the function

$$C(\lambda) = \|x_\lambda\|^2 + 2\lambda^2 \frac{d}{d\lambda^2}\|x_\lambda\|^2 \tag{4}$$

The L-curve criterion involves a log-log scale plot of $\|x\|$ against $\|Ax-b\|$ for all valid regularization parameters. The optimal λ_L lies in the corner of L-curve and can be found as a point of maximal curvature.

2.3. Simulations

The numerical procedures for Tikhonov regularization, L-curve and CRESO computations were implemented based on singular value decomposition (SVD) of transfer matrix A [9]. For the case of zero-order Tikhonov regularization both curvature of L-curve and CRESO function can be computed directly without numerical differentiation.

Modelling errors were introduced into the inverse problem by changing the conductivities of fat, lungs, blood and bones in the finite element model, varying the anisotropy ratio for skeletal muscles and changing model geometry. Geometric errors were simulated by scaling or displacement of the finite element mesh in the region of the heart. The deformation was smoothed with 3D Gaussian distribution centered on the heart and parameterized to confine the deformation in the heart region. The scaling corresponded roughly to +5 *mm* and -5 *mm* variation of the heart radius. The displacement was 10 *mm* and 20 *mm* to the right or to the left. Setting conductivity of bones to average value of 0.1 *S/m* corresponds to the situation when the model is constructed from MRI scans where bones are not resolved. Transfer matrices were computed including modelling errors and used for reconstructing the epicardial potentials from simulated BSPMs gained with the original model. Gaussian noise of 0.5% of torso potential range was added to the BSPMs in all simulations.

The body surface potentials were "measured" at 64 locations of the torso surface and the epicardial potentials were reconstructed at 306 equally spaced epicardial nodes. The positioning of the measurement electrodes was dense at the front of the torso and dispensed in regions more distant to the heart. Such an arrangement allows to improve the condition number of transfer matrix compared to the same number of regularly placed electrodes [10].

In order to evaluate the success of regularization procedure, an optimal solution is required. Although the simulated epicardial potentials were available, they could not be used for direct comparison with reconstructed ones. The reason is that the high frequency content of the realistic simulated patterns is impossible to reconstruct due to limited number of sampling points on epicardial surface and even less number of measurement electrodes. Therefore, the optimal solution was constructed as follows. A transfer matrix $\widetilde{A}$ was computed with about 500 nodes on body surface and the same 306 epicardial nodes as in all other simulations. Optimal solution x^{opt} was found using the truncated pseudoinverse of $\widetilde{A}$:

$$x^{opt} = \widetilde{A}_k^{\dagger} \tilde{b} \tag{5}$$

where $\tilde{b}$ is the vector of the simulated body surface potentials without any added noise, and the truncation parameter k was chosen by minimizing

$$\|Ax^{opt} - b\|_2 \tag{6}$$

A and b being the original transfer matrix and the simulated torso potentials (without added noise) for the 64 electrodes configuration.

The relative error (RE) and the correlation coefficient (CC) were used to compare the reconstructed potential distributions with the optimal ones:

$$RE = \frac{\|x - x^{opt}\|_2}{\|x^{opt}\|_2} \tag{7}$$

$$CC = \frac{\sum_i (x_i - \overline{x})(x_i^{opt} - \overline{x}^{opt})}{\sqrt{\sum_i (x_i - \overline{x})^2}\sqrt{\sum_i (x_i^{opt} - \overline{x}^{opt})^2}} \tag{8}$$

3. Results

The BSPMs were simulated with time a step of 2 *ms* for complete cardiac cycle. Fig. 2 shows the simulated electrocardiogram (ECG) corresponding to the standard lead I. The simulations were carried out as described above. Only the time interval corresponding to the QRS complex (200-250 ms) was considered. To evaluate the performance of L-curve and CRESO criteria, optimal regularization parameter λ_{opt} is found by minimizing the RE between the reconstructed epicardial potentials and optimal solution x^{opt}. The average relative errors $\langle RE_L \rangle$, $\langle RE_C \rangle$ and $\langle RE_{opt} \rangle$ were also computed to characterize the success of the reconstruction procedure on the whole QRS interval. They correspond to L-curve, CRESO and optimal regularization parameter choices, respectively. The values of the average relative errors, the correlation coefficients for three moments of time (Fig. 2) and the values of regularization parameters for several types of modelling errors are summarized in Table 1. Changing the conductivity of fat, lungs or blood by 20% did not lead to any changes of average RE compared to the original model and led to only little changes in the computed optimal regularization parameters.

4. Discussion

Both CRESO and L-curve criteria performed equally well and delivered almost the same values of the optimal regularization parameter for unchanged model and moderate modelling errors, such as changing the conductivity of single tissue classes by up to 20%, little scaling and displacement of the heart region. Under worse conditions, the L-curve criterion appeares to be more stable and still deliveres the regularization parameter close to the optimal. Both criteria were additionally stabilized by setting the limit on minimal valid regularization parameter. This value was constant during the heart cycle and equal for both criteria. The analysis of average RE shows that moderate changes in conductivity of single tissue classes as well as little geometric errors do not lead to significant errors in the reconstructions. The changes in anisotropy ratio and the displacements of the heart geometry have the highest effect on the inverse problem solution. By the displacements to the left the heart is moved closer to the body surface and thus the effect on the inverse solutions is more noticeable compared to the displacements to the right. Since the reconstructions obtained with homogeneous isotropic model had the greatest errors in computed potentials and the lowest correlation with the optimal solution, such model can not be recommended for inverse epicardial potential reconstructions.

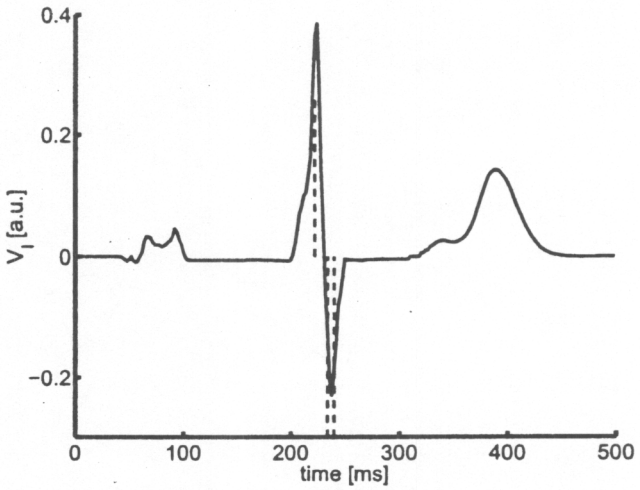

Figure 2. Simulated electrocardiogram. The vertical dashed lines correspond to t=222, 234 and 240 ms.

References

[1] Klepfer RN, Johnson CR, MacLeod RS. The effects of inhomogeneities and anisotropies on electrocardiographic fields: A 3-D finite-element study. IEEE Transactions on Biomedical Engineering Aug. 1997;44(8):706–719.

[2] Pesola K, Jötjönen J, Nenonen J, Magnin IE, Lauerma K, Fenici K, Katila T. The effect of geometric and topologic differences in boundary element models on magnetocardiographic localization accuracy. Helsinki University of Technology Publications in Engineering Physics, 1999.

[3] Sachse FB, Glas M, Müller M, Meyer-Waarden K. Segmentation and tissue-classification of the Visible Man dataset using the computertomographic scans and the thin-section photos. In Proc. First Users Conference of the National Library of Medicine's Visible Human Project. 1996; URL `http://www-ibt.etec.uni-karlsruhe.de/people/fs/vh2.html`.

[4] Werner CD, Sachse FB, Dössel O. Electrical excitation propagation in the human heart. International Journal of Bioelectromagnetism Sep. 2000;2-2. URL `http://www-ibt.etec.uni-karlsruhe.de/cardio2000/werner/index.html`. ISSN 1456-7865.

[5] Henriquez CS. Simulating the electrical behaviour of cardiac tissue using the bidomain model. Critical Reviews in Biomedical Engineering 1993;21(1):1–77.

[6] Hansen PC. Rank-deficient and discrete ill-posed problems. Philadelphia: SIAM, 1998.

[7] Colli-Franzone P, Guerri L, Taccardi B, Viganotti C. Finite element approximation of regularised solutions of the inverse potential problem of electrocardiography and applications to experimental data. Calcolo 1985;XXII(1):91–186.

[8] Hansen P, O'Leary DP. The use of the L-curve in the regularization of discrete ill-posed problems. SIAM Journal on Scientific Computing Nov. 1993;14(6):1487–1503.

[9] Press WH, Teukolsky SA, Vetterling WT, Flannery BP.

Table 1. Results of the epicardial potential reconstructions

tissue	t, ms	$\langle RE_L \rangle$	$\langle RE_C \rangle$	$\langle RE_{opt} \rangle$	CC_L	CC_C	CC_{opt}	$\lambda_L, 10^{-3}$	$\lambda_C, 10^{-3}$	$\lambda_{opt}, 10^{-3}$
original	222	0.824	0.826	0.802	0.762	0.758	0.776	1.33	1.44	0.80
model	234				0.805	0.806	0.806	0.54	0.51	0.51
(muscles 1:3)	240				0.868	0.867	0.867	1.50	1.32	1.39
muscles	222	0.910	1.07	0.840	0.673	0.672	0.674	1.52	1.42	3.44
1:10	234				0.723	0.721	0.695	0.38	0.34	0.37
	240				0.824	0.808	0.829	1.01	0.78	2.77
bones	222	0.831	0.903	0.810	0.752	0.751	0.765	1.17	1.23	0.80
$0.1 S/m$	234				0.803	0.803	0.802	0.51	0.49	0.54
	240				0.860	0.859	0.860	1.50	1.34	1.47
homog.	222	0.892	0.960	0.853	0.596	0.573	0.662	1.25	1.17	3.87
isotrop.	234				0.707	0.422	0.718	2.55	0.15	1.27
	240				0.764	0.719	0.798	1.12	2.06	4.42
scale heart	222	0.821	0.861	0.800	0.782	0.786	0.786	1.29	0.90	0.90
$+5mm$	234				0.803	0.803	0.804	0.61	0.62	0.54
	240				0.857	0.856	0.856	1.68	1.52	1.58
scale heart	222	0.838	0.843	0.813	0.734	0.734	0.750	1.22	1.22	0.76
$-5mm$	234				0.798	0.799	0.791	0.47	0.42	0.66
	240				0.869	0.868	0.869	1.32	1.12	1.30
heart	222	0.832	0.835	0.811	0.752	0.731	0.758	1.48	0.57	1.07
$10mm$ left	234				0.774	0.773	0.777	0.59	0.60	0.52
	240				0.873	0.871	0.873	1.47	1.28	1.44
heart	222	0.836	0.849	0.814	0.747	0.746	0.759	1.27	1.30	0.76
$10mm$ right	234				0.792	0.791	0.790	0.52	0.47	0.66
	240				0.828	0.827	0.829	1.51	1.33	1.55
heart	222	0.861	1.28	0.836	0.718	0.653	0.721	1.79	0.51	1.46
$20mm$ left	234				0.690	0.689	0.687	0.63	0.68	0.73
	240				0.841	0.835	0.843	1.41	1.19	1.68
heart	222	0.868	0.899	0.841	0.710	0.710	0.710	1.28	1.36	1.30
$20mm$ right	234				0.744	0.743	0.742	0.54	0.49	1.05
	240				0.754	0.750	0.762	1.51	1.33	2.41

Numerical Recipes in C. 2 edition. Cambridge, New York, Melbourne: Cambridge University Press, 1992. ISBN 0-521-43108-5.

[10] Dössel O, Schneider FR, Müller M. Optimization of electrode positions for multichannel electrocardiography with respect to electrical imaging of the heart. In Proc. 20th Conf. IEEE Eng. in Med. and Biol. Hong Kong, China, 1998; 71–74.

Address for correspondence:

Dipl.-Phys. Oleg Skipa
Institut für Biomedizinische Technik
Universität Karlsruhe (TH)
Kaiserstr. 12
76131 Karlsruhe, Germany
os@ibt.etec.uni-karlsruhe.de